Sakarya University Journal of Science

ISSN : 2147-835X
Publisher : Sakarya University

Vol. 28, No. 3, 531-541, 2024
DOI: https://doi.org/10.16984/saufenbilder.1352961

Research Article

Design of Sulfur Resistant Cobalt Catalysts by Boron Promotion: Atomic Scale Insights

Ali Can Kızılkaya

İzmir Institute of Technology, Faculty of Engineering, Department of Chemical Engineering, İzmir, Türkiye, alicankizilkaya@iyte.edu.tr

ARTICLE INFO

Keywords:
Boron
Cobalt
Sulfur
Catalysis
Density Functional Theory

Article History:
Received: 31.08.2023
Accepted: 07.03.2024
Online Available: 06.06.2024

ABSTRACT

The effect of boron promotion on atomic sulfur formation by hydrogen sulfide dissociation on Co(111), flat surfaces of cobalt nanoparticles, was investigated using Density Functional Theory calculations. The results show that on clean Co(111), hydrogen sulfide dissociation proceeds fast due to low activation barriers, yielding atomic sulfur on the cobalt surfaces. Boron promotion hinders the dissociation of hydrogen sulfide due to increased activation barriers. Furthermore, boron prevents the interaction of sulfur compounds with cobalt surface atoms, as these poisons bind on boron. The findings indicate that boron is an effective promoter that can be used to design sulfur resistant cobalt catalysts.

1. Introduction

Boron is a crucial element used in several industries ranging from materials and chemistry to defence, energy and medical industries. Türkiye is home to 73% of global boron reserves, based on estimates of Eti-Maden, the Turkish state-owned boron-focused mining company. Therefore, utilizing boron for both existing and novel purposes stands as a strategic choice for Türkiye that can boost its technological development. Boron has been historically utilized based on high-performance glass (mainly fibreglass) making, accounting for ~50% of the global boron consumption.

Among other major uses are the manufacture of plant nutrients in agriculture and also detergents in the chemical industry, but boron- based materials find minor uses in many industries including nuclear, metallurgical, textile, and cosmetic sectors [1]. Furthermore, renewed interest in boron due to its unique electronic and chemical properties [2] have resulted in R&D activities for boron utilization in novel areas. Boron-based materials are researched as therapeutic agents in medical treatments [3], hydrogen storage materials [4], and as heterogeneous catalysts in thermo-, electro- and photo-chemical processes [5], among others.

Among the industries where boron is used, chemical industry is an important component, since it consumes significant amounts of energy, resulting in 19% of all industrial CO_2 emissions [6]. In chemical industry, one of the main current challenges is to make the sector more sustainable, for example via increasing energy efficiency and limiting the formation of waste and by-products. For this purpose, the most reasonable solution is the use of catalysts. Catalysts are used in more than 90% of all chemical processes, delivering significant sustainability benefits [7]. However, catalysts are usually made from rare and precious elements. Due to the growing needs and concerns to make the chemical industry more sustainable, an important area of research is to synthesize catalysts based on more abundant elements [8].

Cite as: A.C. Kızılkaya (2024). Design of Sulfur Resistant Cobalt Catalysts by Boron Promotion: Atomic Scale Insights, *Sakarya University Journal of Science*, 28(3), 531-541. https://doi.org/10.16984/saufenbilder.1352961

In line with this goal of sustainability, catalysts with components that are based on boron have recently been receiving increased attention in academia. A heterogeneous catalyst is made up of three essential components, an active phase, a high area support material and typically a promoter that can boost the activity, selectivity or stability of the catalyst. Boron-based materials were found to have important catalytic properties as active sites in heterogeneous catalysts. Different chemical phases of the boron based catalysts included nitrides, carbides, phosphides and oxides [5]. Boron carbides and phosphides were found to be efficient photocatalysts for water splitting. Carbon nanotubes and graphene that are used as electrocatalysts were found to have increased activity for oxygen reduction reaction (ORR) when coupled with elemental boron. Similarly 1D hexagonal boron nitride (h-BN) sheets also demonstrated high performance for the electrocatalytic OR reaction [5].

The utilization of h-BN sheets in thermal oxidative dehydrogenation of alkanes resulted in numerous studies investigating supported boron-based catalysts for this reaction. Among these, metallic and non-metallic borides and porous materials in the form of boron oxide and boron-phosphorus mixed oxides showed high propylene selectivities in the partial oxidation of propane [9]. Other publications revealed that different types of oxidic supports (such as alumina, magnesia, silica, etc.) can have varying effects on the boron-based active sites and optimization of the support could lead to improved selectivity or stability of the catalysts via boron-support interactions [10].

Boron has also been used as a promoter in several catalytic reactions with different effects. Among the most important examples are boron-doped carbon nanotubes for photocatalytic and electrocatalytic applications [11] and boron-doped iron [12] or cobalt based catalysts [13] for thermal catalytic Fischer-Tropsch Synthesis (FTS). Boron-doped graphene was used as an electrocatalyst with increased activity in fuel cell applications [14], boron doping was found to increase selectivity to ethanol on Cu(111) for carbon dioxide electroreduction [15]. For photocatalytic applications, boron-doped TiO_2 was found to be an effective catalyst for antibiotic degradation [16]. In the area of thermal catalysis, boron was found to be an important promoter that can prevent the deactivation of iron or cobalt based Fischer-Tropsch Synthesis catalysts. On iron catalysts, an experimental study [12] indicated that that boron promotion reduces the rate of deactivation, while in a later study [17] based on DFT modeling, it was found that boron reduces the deactivation rate by blocking the adsorption sites for carbon.

Boron promotion was also investigated for cobalt FTS catalysts. Tan et al. have presented [13] a detailed analysis of the boron promotion related to carbon deposition on cobalt FTS catalysts, based on a combined experimental and computational study. They performed Density Functional Theory (DFT) calculations on both flat and stepped cobalt surfaces to examine the structure of boron promoted cobalt catalysts. Supporting the computational model in this study, they indicated that atomic boron is stable at the hcp site on Co(111) surfaces. Furthermore, they indicated that boron atoms weaken carbon adsorption by withdrawing electronic charge from the cobalt surfaces.

Despite the promising results related to the effect of boron promotion on hindering deactivation by carbon deposition, its effects on sulfur poisoning were rarely investigated. In an experimental study, Li and Coville [18] analyzed the effect of boron on the sulfur poisoning of cobalt FTS catalysts. It was speculated that boron prevents sulfur poisoning via hindering the charge accumulation on cobalt atoms due to sulfur poisoning. However, as their study did not include data related to the chemical and electronic structure of sulfur and boron additives on the catalyst surface, they were unable to provide evidence for the boron promotion mechanism.

In a recent study [19], the potential of boron as a promoter to hinder sulfur poisoning was evaluated on other metal surfaces, including Pd, Pt, Rh and Ru, based on DFT modeling. Similar to this study, they also investigated H2S dissociation on Pd(111) surface. It was concluded that on Pd surfaces boron can act as a promoter to prevent sulfur poisoning by

hindering H_2S dissociation and weakening the binding of atomic sulfur.

Based on the analysis of the literature, it is obvious that boron is used as a promoter to hinder deactivation by coke deposition on cobalt [13] and iron [12]. Furthermore, a recent study also indicated that it can prevent H_2S dissociation on palladium catalysts [19]. Therefore, it is of interest to analyze how H_2S dissociates on cobalt surfaces and how boron promotion effects its dissociation and the adsorption of dissociation products. Up to our knowledge, there are neither experimental nor computational investigations related to H_2S dissociation and how it is affected by boron promotion on the cobalt surfaces.

The aim of this study is to compare the adsorption and dissociation of hydrogen sulfide on clean vs boron promoted cobalt surfaces, in order to evaluate the potential of boron as a promoter for cobalt FTS catalysts to prevent sulfur poisoning. The adsorption of H_2S, its dissociation and the adsorption of dissociation products are investigated with state-of-the-art computational modeling based on DFT calculations. The results indicate that boron can act as an effective promoter for preventing the sulfur poisoning of FTS catalysts as it hinders the dissociation of H_2S and also prevents the interaction of H_2S and the dissociation products with cobalt surface atoms by acting as an adsorption site for sulfur species.

2. Computational Methods

Periodic Density Functional Calculations (DFT) were performed using the Vienna Ab-initio Simulation Package (VASP) [20, 21]. The exchange-correlation energy was calculated with the revised Perdew–Burke–Ernzerhof functional (revPBE) [22] including the non-local vdW–DF correlation [23-26]. The use of vdW-DF functional allows us to predict accurately model adsorption of molecules with low adsorption energies that bind on surfaces mainly via van-der-Waals interactions such as H_2S. The surfaces were cut from a bulk fcc-Co structure with a lattice parameter of 3.56 Å, optimized with the vdW-DF functional. The calculated lattice parameter is matches very well with the experimental value of 3.55 Å [27].

The electron-ion interaction was modeled by the projector-augmented wave (PAW) method [28]. Spin-polarized calculations were performed to account for the magnetic properties of cobalt with a plane wave cut-off energy of 400 eV. Surface terraces of face-centered-cubic (fcc) Co nanoparticles were modeled with 4 atomic layers-thick Co(111) slab models with a p(2x2) unit cell. The adsorption of H_xS (x=2,1,0) species in this unit cells corresponds to a coverage of 25% of the surface cobalt atoms with adsorbates, in other words, a surface coverage of 0.25 monolayer (ML).

The atoms at the bottom 2 layers half of the slabs in the z-direction were kept fixed at their pre-optimized positions, while all other atoms were allowed to relax during optimization calculations. The reciprocal space was sampled with a (5×5×1) k-points grid automatically generated using Monkhorst-Pack method [29]. A vacuum height of 15 Å was inserted between slabs to avoid coupling between successive slabs in the z-direction. Dipole corrections in z-direction were used for all optimizations. The structural models were optimized until all the forces acting on atoms are smaller than 0.02 eV/Å.

The binding (adsorption) energies (E_{ad}) of surface species (adsorbates) are calculated based on the formula:

$$E_{ad} = E_{slab\_ad} - E_{slab} - E_{ad\_vac} \quad (1)$$

where Eslab_ad represents the energy of the optimized system of adsorbate on the slab, Eslab represents the energy of the clean slab (without the adsorbate) and Ead_vac represents the energy of the adsorbate molecule in a vacuum. The reaction energies (RE) were calculated after the optimization of initial states (IS) and final states (FS) of the reactions, based on the following formula:

$$RE = E_{FS} - E_{IS} \quad (2)$$

After initial and final states are calculated, the transition states were optimized by CI-NEB [30] method until the forces acting on the image with the highest energy are lower than 0.04 eV/Å . All transition states were further confirmed by

vibrational frequency analysis, which indicated a single imaginary vibrational frequency for them. During the vibrational frequency analysis, the atoms were displaced from their equilibrium positions by 0.015 Å. After the identification of TS structures, the activation barriers (Ea) are calculated based on the formula:

$$E_a = E_{TS} - E_{IS} \quad (3)$$

3. Results and Discussion

3.1. H_2S adsorption and dissociation on Co(111)

Sulfur poisoning on cobalt surfaces was previously ascribed to atomic sulfur species, based on experimental and computational surface science studies [31]. Therefore, adsorption of H_2S on Co(111) surface and its successive dissociation to atomic sulfur species is investigated. H_2S decomposition on metal surfaces occurs via stepwise dehydrogenation yielding first SH and then atomic S species.To calculate the activation barriers with DFT modeling, first, initial and final states for H_2S and SH dissociation reaction should be optimized.

Therefore, optimal adsorption configurations of H_2S, SH and S, i.e. H_xS (x=2,1,0), species on Co (111) surface are calculated. There are 4 different adsorption sites on Co(111), namely the 4-fold hollow (hcp) site, 3-fold hollow site (fcc), bridge site and the top site. These adsorption sites are shown in Figure 1, based on the adsorption of atomic sulfur in each site.

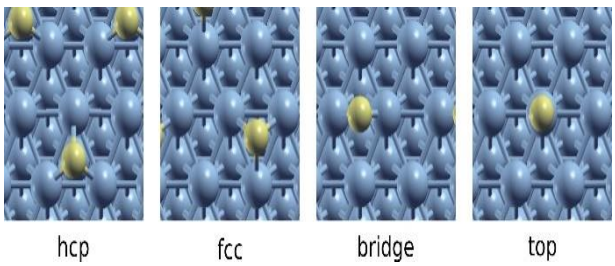

Figure 1. Different adsorption sites on Co(111), a) hcp, b)fcc, c) bridge and d) top (S atoms are shown to illustrate the adsorption sites clearly)

In order to identify the optimal adsorption configuration for the H_xS species, each adsorbate is optimized in all 4 different adsorption sites. Adsorption energies of H_xS species on different adsorption sites on Co(111) are listed in Table 1.

Table 1. The adsorption energies of H_xS species (kJ/mol) on different adsorption sites on Co(111) (NA indicates that adsorption of the indicated species is not possible on the specific site)

	hcp	fcc	bridge	top
H_2S	NA	NA	NA	-43
SH	-255	-258	NA	NA
S	-471	-493	NA	NA

The adsorption geometry with the minimum adsorption energy is the preferred, i.e., energetically the most stable, adsorption configuration, which indicates the experimentally observed adsorption site under identical surface structures and vacuum conditions. The preferred adsorption configurations of H_2S, SH and S species are shown in Figure 2.

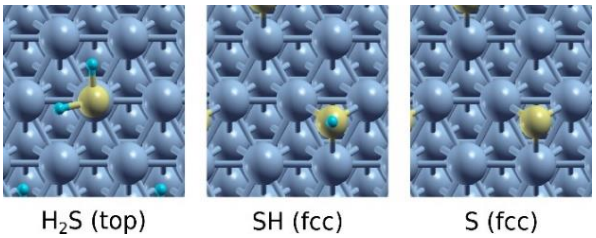

Figure 2. The preferred (most stable) adsorption sites and geometries of H_xS species on Co(111)

The results show that H_2S adsorption can only occur on the top sites, similar to what has been reported on several other transition metal surfaces [32]. For both SH and S species, adsorption occurs on the hollow sites, while adsorption at the fcc site is more stable for both species. A previous study has indicated that SH adsorption is most stable at the bridge sites while S adsorption occurs preferentially at the fcc sites on transition metals like Ni and Ru 32]. Our results indicate that S adsorption is similar on cobalt with other transition metals, while SH adsorption is different as it occurs on the fcc hollow sites, compared to the bridge sites on metals like Ni and Ru. The adsorption energies of SH and S species are calculated as -258 and -493 kJ/mol respectively, indicating that both of these species are strongly chemisorbed on Co(111) surface.

After the identification of the preferred adsorption sites for H_xS species, initial and final state configurations for reactions are optimized on Co(111). For the initial and final states that involve coadsorption of the species (such as the

final state of H_2S dissociation involving SH and H), all possible coadsorption configurations were investigated and the geometry with the minimum energy is used as the initial/final state of the reaction. Based on the optimized initial state (IS) and final state (FS) configurations, transition state (TS) geometries were obtained based on CI-NEB calculations. The IS, TS and FS structures for H_2S decomposition reactions are shown in Figure 3.

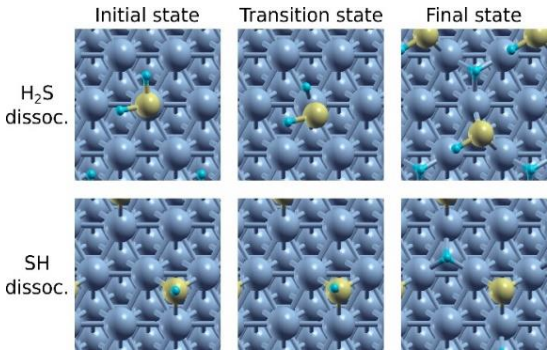

Figure 3. The IS, TS and FS structures for H_2S dissociation reactions on Co(111)

Based on the TS obtained for the reactions, activation barriers are obtained for the dissociation reactions. Similarly, the reaction energies are calculated based on the energy difference of the final state (FS) and initial state (IS). Based on the IS, TS and FS configurations shown in Figure 3, the kinetic parameters of H_2S dissociation to atomic S on Co(111) are calculated, as shown in Table 2.

Table 2. The activation barriers (E_a) and the reaction energies (RE) (kJ/mol) for H_2S and SH dissociation on Co(111)

	E_a	RE
$H_2S \rightarrow SH + H$	33	-94
$SH \rightarrow S + H$	7	-105

The data in Table 2 indicates that H_2S decomposition to HS and S have low barriers, which will result in fast dissociation of H_2S to atomic S under FTS reaction conditions. Our results are in line with the experimental findings that H_2S readily decomposes to atomic S on Co(0001) single crystal surfaces at low temperatures and that atomic S deposits were observed on Co(0001) surfaces after exposure of Co(0001) surface to FTS reactants of CO and H_2 in the presence of H_2S under applied pressure and temperature conditions [31].

3.2. H_2S adsorption and decomposition on boron covered Co(111)

Boron adsorption is investigated on all possible (hcp, fcc, bridge and top) adsorption sites of the Co(111) surface. Among these configurations, boron adsorption is only possible at the hcp and fcc hollow sites. Among these two sites, hcp is the most stable adsorption site with an E_{ad} of 492 kJ/mol and boron adsorption at the hcp site is 11 kJ/mol more stable compared to the adsorption at fcc site. These results are in line with the literature, where boron adsorption was reported to be most stable at the hcp site on Co(111) [13], [33]. Boron adsorbed at the most stable hcp site on the Co(111) surface is shown in Figure 4.

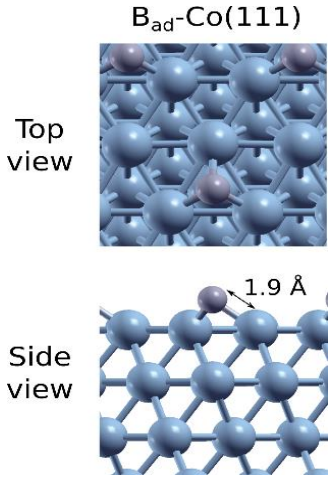

Figure 4. Top and side views of boron adsorbed at the most stable hcp site on Co(111)

Boron promotion results in the formation of adsorption sites on boron covered Co(111) [B-Co(111)] that are close to the boron atom, and sites that are far away from boron, as shown in Figure 5.

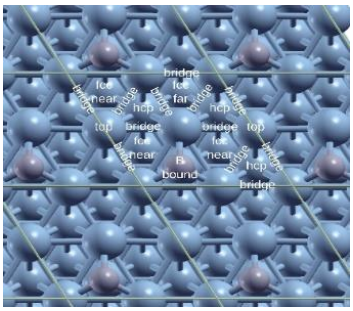

Figure 5. The adsorption sites on the B-Co(111) surface

Figure 5 shows that on B-Co(111), two different types of fcc sites are present, the ones that are near and far from B. There are single types of hcp, bridge and top sites, similar to the case of clean Co(111). Interestingly, H_xS species can also adsorb on boron atoms without interacting with the surface cobalt atoms, as shown in B-bound adsorption site on B-Co(111) in Figure 5. The adsorption of H_xS species were investigated in all adsorption sites shown on B-Co(111) and the results are shown in Table 3.

Table 3. The adsorption energies of H_xS species (kJ/mol) on different adsorption sites on B-Co(111)

	hcp	fcc-near	fcc-far	bridge	top	B-bound
H_2S	-29	NA	-29	NA	-29	-36
SH	NA	NA	-169	-235	NA	-329
S	NA	NA	-437	NA	NA	-482

On B-Co(111), most stable adsorption sites for H_xS adsorption are located where the species are B-bound, i.e. bonded to surface boron atoms. H_xS adsorption at sites that are away from B, where they interact only with Co atoms at the surface are found to have lower E_{ad} values. The preferred adsorption sites for H_xS species, bound to boron atoms on B-Co(111), are shown in Figure 6.

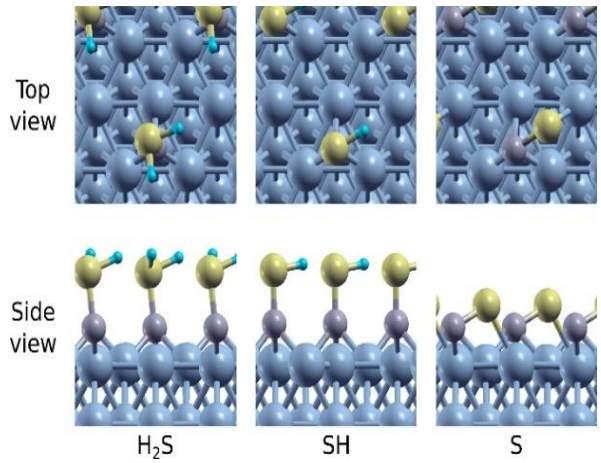

Figure 6. The preferred (most stable) adsorption sites and geometries for HxS species on B-Co(111)

The results shown in Table 3 and Figure 6 allow to draw important conclusions related to the effect of boron on H_xS adsorption on Co(111). When Co(111) surface is covered with boron, the binding of H_2S, SH and S species are significantly stronger when they occur bound to B atoms, compared to their adsorption on cobalt atoms of B-Co(111) surface. To understand how boron effects the adsorption energies of H_xS with respect to the clean Co(111) surface, adsorption energies of H_xS species are compared for both surfaces, as shown in Table 4.

Table 4. Comparison of adsorption energies of H_xS species (kJ/mol) on Co(111) vs B-Co(111) surfaces

	Co(111)	B-Co(111) [B-bound]	B-Co(111) [Co-bound]
H_2S	-43	-36	-29
SH	-258	-329	-235
S	-493	-482	-437

Table 4 shows that on the boron covered B-Co(111) surface, H_xS adsorption at sites that are away from boron, results in H_xS adsorption energies that are even lower compared to the ones on clean Co(111). Overall, these finding show that boron atoms will act as H_xS sinks on the Co(111) surface, i.e. H_xS species will bind preferentially on B atoms instead of surface cobalt atoms. As a result, boron promotion will hinder the adsorption of H_xS species on the metallic cobalt surface, resulting in significantly lower H_xS coverages on the catalyst surface. In order to understand how boron promotion effects H_2S dissociation to atomic S, IS, TS and FS configurations were optimized for H_2S and SH dissociation reactions, as shown in Figure 7.

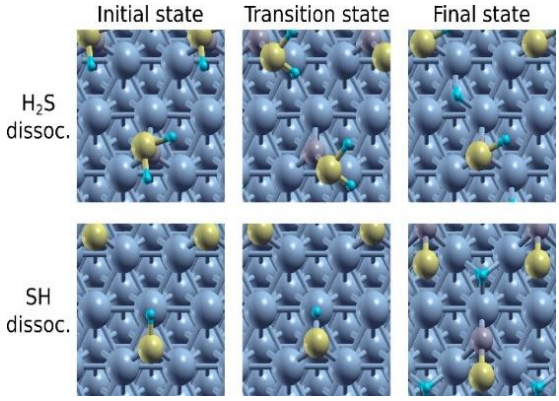

Figure 7. IS, TS and FS structures for H_2S and SH dissociation on B-Co(111)

Figure 7 indicates that the dissociation of H_2S yields SH species bound to boron, while the H atom is located on the cobalt surface. This shows that SH produced as a result of H_2S dissociation will be bound to boron atoms and not interact with cobalt atoms. Similarly, SH dissociation also produces S atoms that are bound to boron, having no interaction with cobalt atoms. Nevertheless, it is also important to investigate if the SH and S species that are produced as a result of dissociation reactions and bound to boron can migrate to their less stable adsorption sites where

they are bound to carbon atoms. Therefore, the kinetic parameters of both H_xS dissociation from the most stable B-bound adsorption sites and their migration to surface cobalt atoms and successive dissociation are investigated and summarized in Table 5.

Table 5. The activation barriers (E_a) and the reaction energies (RE) (kJ/mol) of H_xS dissociation and H_xS migration reactions on B-Co(111) surface

	E_a	RE
H_2S_B_bound → SH_B_bound + H	7	-146
H_2S_Co_bound → SH_fcc_far + H	NA	NA
SH_B_bound → S_B_bound + H	74	-18
SH_B_bound → SH_bridge	108	94
S_B_bound → S_fcc_far	82	45

Table 5 shows a clear effect of boron promotion on Co(111) surface related to H_2S and SH dissociation. H_2S species can dissociate easily to SH with a very low barrier of 7 kJ/mol starting from their preferred B-bound configuration. However, this dissociation will yield SH species that are not interacting with cobalt atoms but instead bound to B atoms, pointing away from the surface. In order to produce SH species on the cobalt surface, the dissociation of H_2S bound to the cobalt surface atoms (i.e. away from B, located on top, fcc or hcp adsorption sites) have to occur. However, the results indicated that this pathway cannot occur, as during the dissociation process SH species get bonded to boron atoms and thus cannot reach the cobalt surface. Therefore, the results indicate that H_2S dissociation on B-Co(111) can only occur on boron atoms and not on the surface cobalt atoms.

SH that is produced as a result of H_2S dissociation is preferentially located on boron atoms. These B-bound SH species can either dissociate to B-bound atomic S or can migrate to the bridge adsorption sites where it is bonded to cobalt atoms. The comparison of kinetic parameters for these two competing pathways show that the dissociation of SH to B-bound atomic S is kinetically favored as it has a lower (74 kJ/mol) activation barrier compared to its migration to bridge site with an activation barrier of 108 kJ/mol. These results show that SH dissociation will proceed on B-Co(111) surface to yield atomic S bonded to boron.

An important consideration related to atomic sulfur on B-Co(111) is related to its migration from the most stable B-bound adsorption site to the fcc_far adsorption sites where it interacts directly with surface cobalt atoms. The results showed that this migration is endothermic with a sizeable activation barrier of 82 kJ/mol. Therefore, the analysis also shows that atomic S that is produced on the B-Co(111) surface will remain bonded to boron atoms and therefore atomic boron will act as a sulfur sink that keeps the metallic cobalt atoms free from sulfur poisoning. In order to further clarify the promotional effect of boron on Co(111) related to sulfur poisoning, the kinetic parameters of H_2S dissociation is compared on clean Co(111) vs B-Co(111) in Table 6.

Table 6. The activation barriers (E_a) and reaction energies (RE) (kJ/mol) of H_2S and SH dissociation on Co(111) vs B-Co(111)

	Co(111)		B-Co(111) [B-bound]		B-Co(111) [Co-bound]	
	E_a	RE	E_a	RE	E_a	RE
H_2S → SH + H	33	-94	7	-146	NA	NA
SH → S + H	7	-105	74	-18	133	111

Table 6 indicates that on clean Co(111), H_2S dissociation to atomic S occurs rapidly due to low activation barriers of 33 kJ/mol and 7 kJ/mol of H_2S and SH dissociations, respectively. As a result of the dissociation, metallic cobalt atoms are covered with atomic S and therefore catalyst surface is poisoned and deactivated. The low activation barriers for dissociation explain why cobalt nanoparticles can easily get poisoned by even low concentrations of H_2S in the gas atmosphere.

On boron covered Co(111), the situation is remarkably different. H_2S adsorption occurs preferentially on the B atoms and not interacting with the cobalt atoms, while H_2S dissociation can occur easily on B atoms, with an even lower activation barrier than the clean Co(111) surface. However, H_2S dissociation cannot occur on the metallic cobalt surface. Furthermore, the dissociation product of SH will be located on

boron atoms with no effect on surface cobalt atoms, just like the case of H_2S adsorption. From this state of SH atoms adsorbed on boron, in order for atomic S to be formed on surface cobalt atoms, SH species has to first migrate to the surface cobalt atoms and dissociate, which is a highly endothermic reaction with a high overall activation barrier of 133 kJ/mol. Therefore, only atomic S bound to boron can form as a result of SH dissociation with an activation barrier of 74 kJ/mol. A comparison of SH dissociation on clean vs boron promoted Co(111) also shows that the activation barrier on B-Co(111) is 67 kJ/mol higher compared to the clean Co(111), which indicates that the rate of atomic S formation on boron promoted Co(111) will be significantly lower compared to the one on clean Co(111).

Overall, the findings in this study indicate that boron is an effective promoter for cobalt based FTS catalysts which can hinder deactivation by sulfur poisoning. The promotional effect of boron stems from the fact the sources of atomic S, the species that is responsible for catalyst poisoning, H_2S and SH species can only be adsorbed on boron atoms and not the surface cobalt atoms, on a cobalt surface that is promoted by boron. Furthermore, the formation of atomic S from SH is significantly slowed down due to an increase in the activation barrier for dissociation. Similar to H_2S and SH, atomic S species will prefer adsorption on boron atoms without being able to interact with surface cobalt atoms. Therefore, our study highlights important molecular scale insights about how boron promotion effectively suppresses the sulfur poisoning of the cobalt FTS catalysts. These findings can pave the way towards the design of more stable and poison-resistant heterogeneous catalysts based on fundamental understanding.

4. Conclusion

In order to investigate the potential of boron promotion in preventing sulfur poisoning of cobalt FTS catalysts, molecular modeling of H_2S decomposition based on periodic DFT was performed on clean and boron promoted Co(111) surfaces, atomically flat terraces, the most stable surface that is found in highest concentration on fcc-cobalt nanoparticles. The main conclusions of the study can be summarized as follows:

1) H_2S dissociation occurs on Co(111) via stepwise dissociation of H_2S to first SH and finally to atomic S species. On non-promoted, clean Co(111), both dissociation reactions are exothermic, with low activation barriers of 33 and 7 kJ/mol for H_2S and SH dissociation respectively. These results explain why cobalt catalysts are rapidly poisoned by sulfur at even low concentrations of gas phase H_2S.

2) On boron promoted Co(111), [B-Co(111)], the adsorption of H_2S, SH and S are all more stable on boron atoms compared to their adsorption on surface cobalt atoms. The adsorption energies of H_xS species on the cobalt atoms of B-Co(111) are significantly lower compared to the ones on clean Co(111). These results show that B atom act as sinks for H_xS species, clearing the cobalt surface atoms from the sulfur species.

3) On B-Co(111), H_2S dissociation can only occur with H_2S species bound to boron and produces SH species that are also B-bound. SH species that are adsorbed on boron atoms cannot migrate to surface cobalt atoms due to an high activation barrier of 108 kJ/mol. Instead, SH dissociation to atomic S on B-Co(111) also occurs on B-atoms, with a 67 kJ/mol higher activation barrier compared to the clean Co(111).

4) Boron can act as an effective promoter that hinders the deactivation of cobalt catalysts via sulfur poisoning, based on fundamental insights obtained by molecular modelling. This study demonstrates how fundamental understanding can be used to screen promoters for heterogeneous catalysts and therefore acts as a guide for future studies related to rational design of more stable solid catalysts.

Article Information Form

Funding
The author has not received any financial support for the research, authorship or publication of this study.

Authors' Contribution
The author contributed fully to the study.

The Declaration of Conflict of Interest/ Common Interest

No conflict of interest or common interest has been declared by the authors.

The Declaration of Ethics Committee Approval

This study does not require ethics committee permission or any special permission.

The Declaration of Research and Publication Ethics

The authors of the paper declare that they comply with the scientific, ethical and quotation rules of SAUJS in all processes of the paper and that they do not make any falsification on the data collected. In addition, they declare that Sakarya University Journal of Science and its editorial board have no responsibility for any ethical violations that may be encountered, and that this study has not been evaluated in any academic publication environment other than Sakarya University Journal of Science.

References

[1] D. M. Schubert, "Borates in Industrial Use BT - Group 13 Chemistry III: Industrial Applications," H. W. Roesky, D. A. Atwood, Eds. Berlin, Heidelberg, Germany: Springer Berlin Heidelberg, 2003, pp. 1–40.

[2] Z. Huang, S. Wang, R. D. Dewhurst, N. V. Ignatev, M. Finze, H. Braunschweig, "Boron: Its Role in Energy-Related Processes and Applications," Angewandte Chemie- International Edition, vol. 59, no. 23, pp. 8800–8816, 2020.

[3] B. C. Das, P. Thapa, R. Karki, C. Schinke, S. Das, S. Kambhampati, S. K. Banerjee, P.V. Veldhuizen, A. Verma, L. M. Weiss, T. Evans, "Boron chemicals in diagnosis and therapeutics," Future Medicinal Chemistry, vol. 5, no. 6, pp. 653–676, 2013.

[4] T. Umegaki, J. M. Yan, X. B. Zhang, H. Shioyama, N. Kuriyama, Q. Xu, "Boron- and nitrogen-based chemical hydrogen storage materials," International Journal of Hydrogen Energy, vol. 34, no. 5, pp. 2303–2311, 2009.

[5] Y. Fang X. Wang, "Metal-Free Boron-Containing Heterogeneous Catalysts," Angewandte Chemie - International Edition, vol. 56, no. 49, pp. 15506–15518, 2017.

[6] I. Eryazici, N. Ramesh, C. Villa, "Electrification of the chemical industry—materials innovations for a lower carbon future," MRS Bulletin, vol. 46, no. 12, pp. 1197–1204, Dec. 2021.

[7] I. Chorkendorff J. W. Niemantsverdriet, Concepts of Modern Catalysis and Kinetics, 3rd Edition, Weinheim, Germany: Wiley-VCH Verlag, 2017, pp 1-21.

[8] D. S. Su, J. Zhang, B. Frank, A. Thomas, X. Wang, J. Paraknowitsch, R. Schlögl, "Metal-Free Heterogeneous Catalysis for Sustainable Chemistry," ChemSusChem, vol. 3, no. 2, pp. 169–180, Feb. 2010.

[9] X. Gao, M. Liu, Y. Huang, W. Xu, X. Zhou, S. Yao, "Dimensional Understanding of Boron-Based Catalysts for Oxidative Propane Dehydrogenation: Structure and Mechanism," ACS Catalysis, vol. 13, pp. 9667–9687, 2023.

[10] W. D. Lu, B. Qiu, Z. K. Liu, F. Wu, A. H. Lu, "Supported boron-based catalysts for oxidative dehydrogenation of light alkanes to olefins," Catalysis Science and Technology, vol. 13, no. 6, pp. 1696–1707, 2023.

[11] D. Jana, C. L. Sun, L. C. Chen, K. H. Chen, "Effect of chemical doping of boron and nitrogen on the electronic, optical, and electrochemical properties of carbon nanotubes," Progress in Materials Science, vol. 58, no. 5, pp. 565–635, 2013.

[12] H. Wan, M. Qing, H. Wang, S. Liu, X. W. Liu, Y. Zhang, H. Gong, L. Li, W. Zhang, C. Song, X. D. Wen, Y. Yang, Y. W. Li, "Promotive effect of boron oxide on the iron-based catalysts for Fischer-Tropsch synthesis," Fuel, vol. 281, no. 1, pp. 118714–118723, 2020.

[13] K. F. Tan, J. Chang, A. Borgna, M. Saeys, "Effect of boron promotion on the stability of cobalt Fischer-Tropsch catalysts," Journal of Catalysis, vol. 280, no. 1, pp. 50–59, 2011.

[14] M. S. Yazıcı F. G. B. San, "Bor doplu CVD grafen üretimi ve yakıt pili performansı," Journal of Boron, vol. 4, no. 3, pp. 141–147, 2019.

[15] J. S. Wang, G. C. Zhao, Y. Q. Qiu, C. G. Liu, " Strong Boron–Carbon Bonding Interaction Drives CO_2 Reduction to Ethanol over the Boron-Doped Cu(111) Surface: An Insight from the First-Principles Calculations ," Journal of Physical Chemistry C, vol. 125, pp. 572–582, 2021.

[16] E. B. Şimşek, "Doping of boron in TiO_2 catalyst: Enhanced photocatalytic degradation of antibiotic under visible light irradiation," Journal of Boron, vol. 2, no. 1, pp. 18–27, 2017.

[17] H. Zhao, H. Jiang, M. Cheng, Q. Lin, Y. Iv, Y. Xu, J. Xie, J. Liu, Z. Men, D. Ma, "Boron adsorption and its effect on stability and CO activation of χ-Fe_5C_2 catalyst: An ab initio DFT study," Applied Catalysis A General, vol. 627, no. August, pp. 118382–118391, 2021.

[18] J. Li N. J. Coville, "Effect of boron on the sulfur poisoning of Co/TiO_2 Fischer-Tropsch catalysts," Applied Catalysis A General, vol. 208, no. 1–2, pp. 177–184, 2001.

[19] A. Almofleh H. A. Aljama, "Boron Doping to Limit Sulfur Poisoning on Metal Catalysts," ChemCatChem, vol. 202201545, pp. 1–8, 2023.

[20] G. Kresse J. Hafner, "Ab initio molecular dynamics for liquid metals," Physical Review B, vol. 47, no. 1, pp. 558–561, Jan. 1993.

[21] G. Kresse J. Furthmuller, "Efficient iterative schemes for ab initio total-energy calculations using a plane-wave basis set," Physical Review B, vol. 54, no. 16, pp. 11169–11186, 1996.

[22] J. P. Perdew, K. Burke, M. Ernzerhof, "Generalized gradient approximation made simple," Physical Review Letters, vol. 77, no. 18, pp. 3865–3868, 1996.

[23] M. Dion, H. Rydberg, E. Schroder, D. C. Langreth, B. I. Lundqvist, "Van der Waals density functional for general geometries," Physical Review Letters, vol. 92, no. 24, pp. 246401–246412, 2004.

[24] G. Roman-Perez J. M. Soler, "Efficient Implementation of a van der Waals Density Functional: Application to Double-Wall Carbon Nanotubes," Physical Review Letters, vol. 103, no. 9, pp. 096102–096109, 2009.

[25] J. Klimes, D. R. Bowler, A. Michaelides, "Chemical accuracy for the van der Waals density functional," Journal of Physics-Condensed Matter, vol. 22, no. 2, pp. 022201–022209, 2010.

[26] J. Klimes, D. R. Bowler, A. Michaelides, "Van der Waals density functionals applied to solids," Physical Review B, vol. 83, no. 19, pp. 195131–195138, 2011.

[27] C. Chen, Q. Wang, G. Wang, B. Hou, L. Jia, D. Li, "Mechanistic insight into the C_2 hydrocarbons formation from Syngas on fcc-Co(111) surface: A DFT study," Journal of Physical Chemistry C, vol. 120, no. 17, pp. 9132–9147, 2016.

[28] P. E. Blochl, "Projector Augmented-Wave Method," Physical Review B, vol. 50, no. 24, pp. 17953–17979, 1994.

[29] H. J. Monkhorst J. D. Pack, “Special Points For Brillouin-Zone Integrations,” Physical Review B, vol. 13, no. 12, pp. 5188–5192, 1976.

[30] G. Henkelman, B. P. Uberuaga, H. Jonsson, “A climbing image nudged elastic band method for finding saddle points and minimum energy paths,” Journal of Chemical Physics, vol. 113, no. 22, pp. 9901–9904, 2000.

[31] Y. Daga A. C. Kizilkaya, “Mechanistic Insights into the Effect of Sulfur on the Selectivity of Cobalt-Catalyzed Fischer–Tropsch Synthesis: A DFT Study,” Catalysts, vol. 12, no. 4, pp. 425–441, 2022.

[32] D. R. Alfonso, “First-principles studies of H_2S adsorption and dissociation on metal surfaces,” Surface Science, vol. 602, no. 16, pp. 2758–2768, 2008.

[33] R. Zhang, H. Liu, Q. Li, B. Wang, L. Ling, D. Li, “Insight into the role of the promoters Pt, Ru and B in inhibiting the deactivation of Co catalysts in Fischer-Tropsch synthesis,” Applied Surface Science, vol. 453, pp. 309–319, 2018.